Supplementary Figures, Tables and legends

CBP modulates dasatinib sensitivity in pre-BCR+ acute lymphoblastic leukemia

Jesús Duque-Afonso[1,5#], Chiou-Hong Lin[1#], Kyuho Han[2], David W. Morgens[2], Edwin E. Jeng[2], Ziming Weng[1,4], Johan Jeong[1], Stephen Hon-Kit Wong[1], Li Zhu[1], Michael C. Wei[3], Hee-Don Chae[3], Martin Schrappe[6], Gunnar Cario[6], Justus Duyster[5], Kathleen M. Sakamoto[3], Michael C. Bassik[2], and Michael L. Cleary[1*]

Affiliations

[1] Department of Pathology, Stanford University School of Medicine, Stanford, CA 94305
[2] Department of Genetics, Stanford University School of Medicine, Stanford, CA 94305
[3] Department of Pediatrics, Stanford University School of Medicine, Stanford, CA 94305
[4] Stanford Center for Genomics and Personalized Medicine, Stanford, CA 94305
[5] Department of Hematology and Oncology, University Medical Center Freiburg, Freiburg, Germany
[6] Department of Pediatrics, University Medical Center Schleswig-Holstein, Campus Kiel
[#] These authors contributed equally to this work

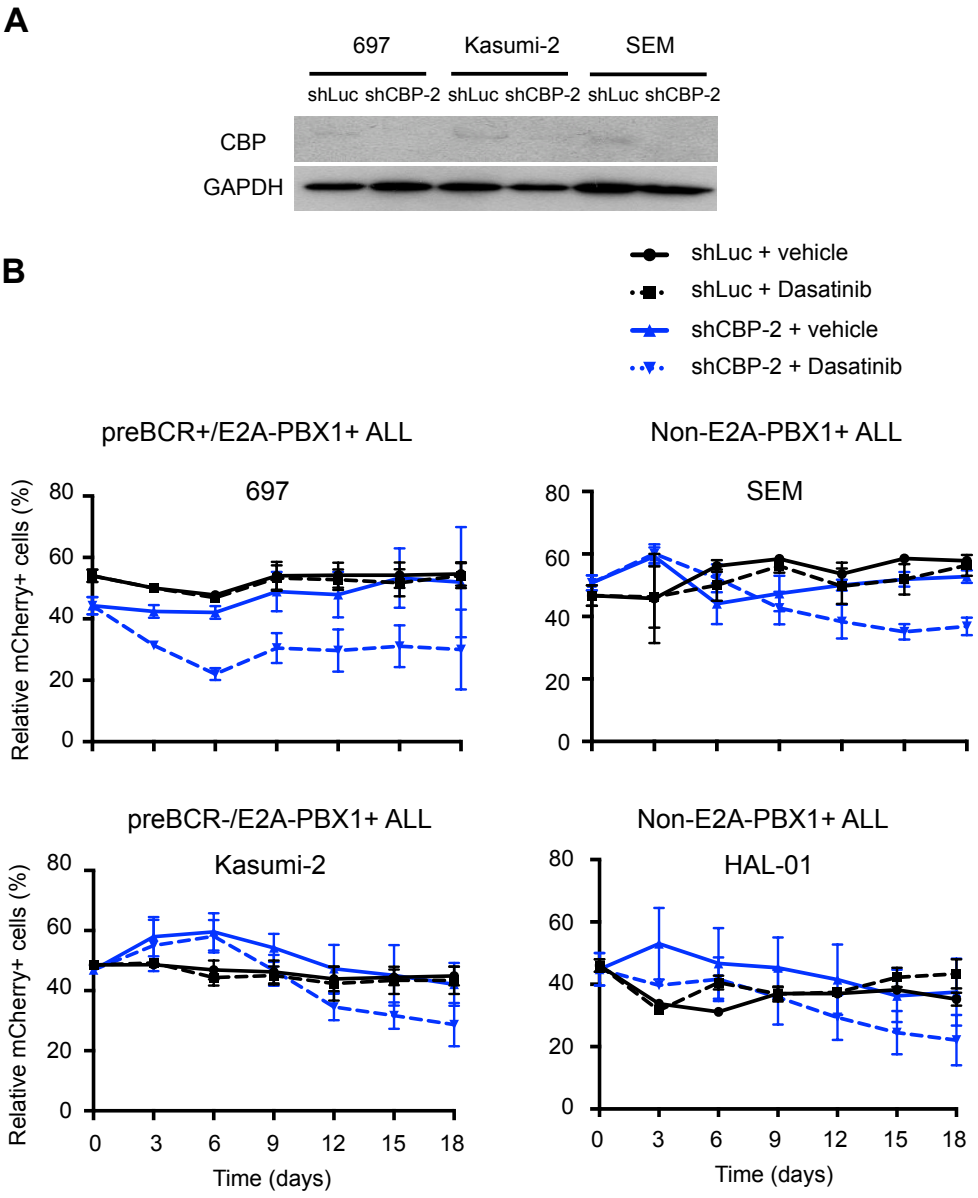

Supplementary Figure S1. CBP modulates sensitivity to dasatinib. (A) Western blot shows CBP levels following single shRNA-mediated knock-down in 697, Kasumi-2 and SEM cell lines. HAL-01 cells do not express CBP and served as a control (data not shown). GAPDH was used as loading control in Western blot. **(B)** Diagram shows percentage of mCherry+ cells transduced with shRNAs for luciferase (control) or CBP in the presence of vehicle or dasatinib (1 μM) for 18 days in human E2A-PBX1+ and non-E2A-PBX1 ALL cell lines. 697 cells were treated with 500 nM dasatinib due to toxicity. Graph show mean ±SEM of three independent experiments.

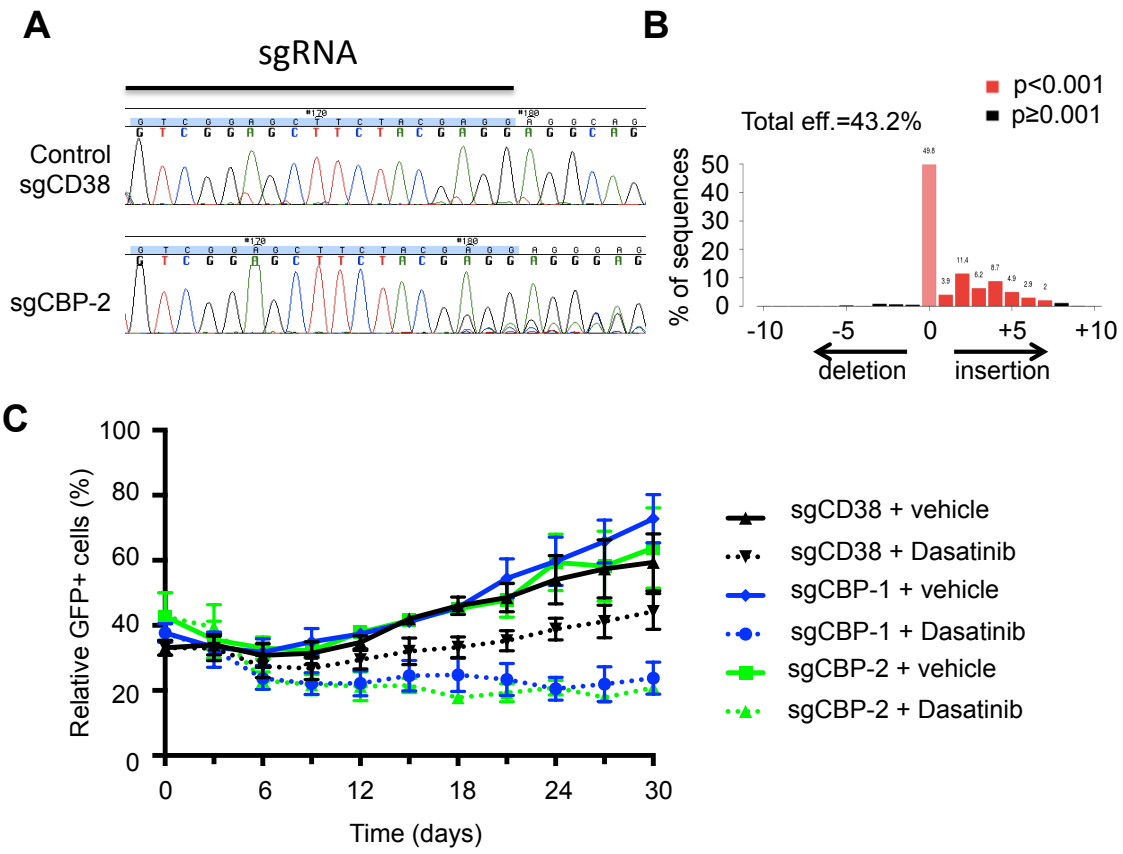

Supplementary Figure S2. Genetic inactivation of CBP increases sensitivity to dasatinib (A) RCH-ACV cells were stably transduced with LentiCas9-Blast-vector and transiently co-transduced with vectors containing sgRNA (pU6-sgRNA EF1Alpha-puro-T2A-GFP lentiviral) sequences for *CD38* (control) or *CBP* genes. Sanger sequencing chromatograms show indels six days after sgRNA-transduction in RCH-ACV cells. **(B)** Genome editing efficiency on *CBP* exon 1 was measured by TIDE assay. A representative experiment is shown. **(C)** Percentage of GFP+ cells transduced with sgRNA for *CD38* (control) or *CBP* in the presence of vehicle or dasatinib (20 nM) for 30 days. Data represent the mean ±SEM of three independent experiments.

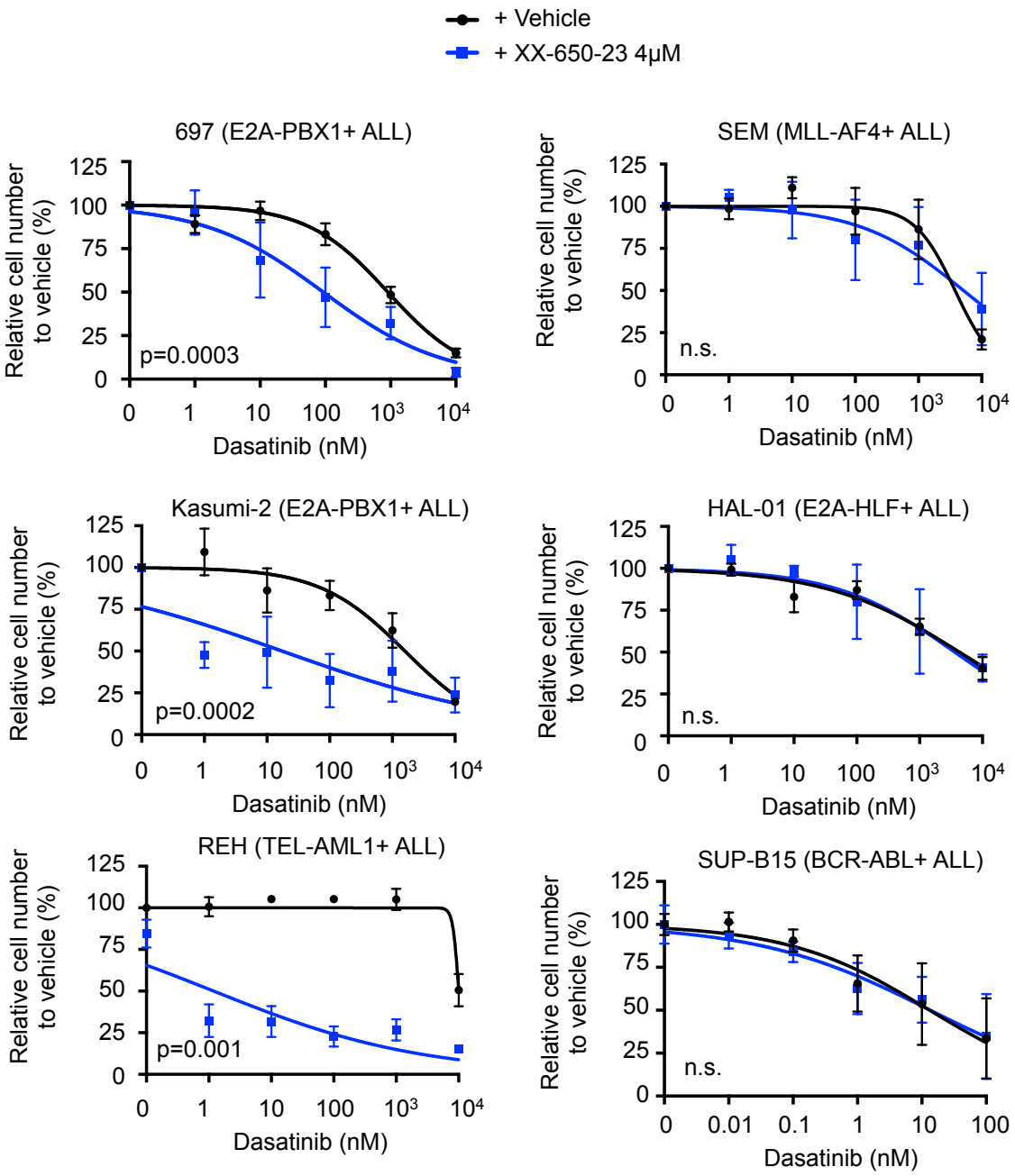

Supplementary Figure S3. Pharmacologic inhibition of CBP increases sensitivity to dasatinib. Titration curves are shown for human ALL cell lines 697, Kasumi-2, REH, SEM and HAL-01 treated with dasatinib in combination with vehicle or XX-650-23 at 4 μM. SUP-B15 (BCR-ABL+) cell line was treated with dasatinib at lower concentration in combination with XX-650-23 at 2 μM due to toxicity. Data represent mean ±SEM of three independent experiments. Statistical analysis by F test.

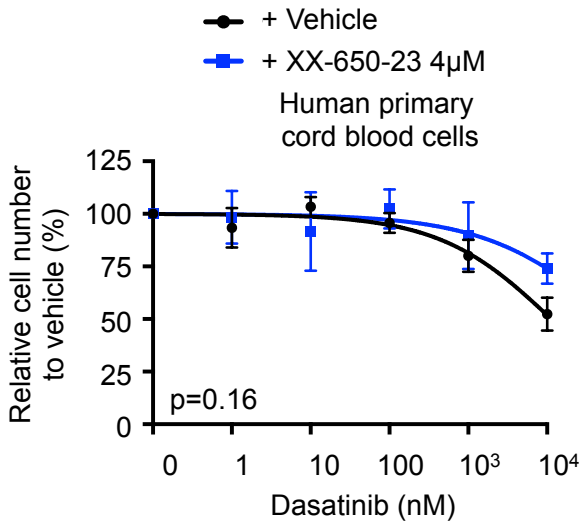

Supplementary Figure S4. Pharmacologic inhibition of CBP with and without dasatinib is not toxic for normal hematopoietic cord blood cells. Titration curve is shown for human cord blood cells cultured with dasatinib in combination with vehicle or XX-650-23 (4 μM). Data represent mean ±SEM of three independent experiments. Statistical analysis was performed by F test.

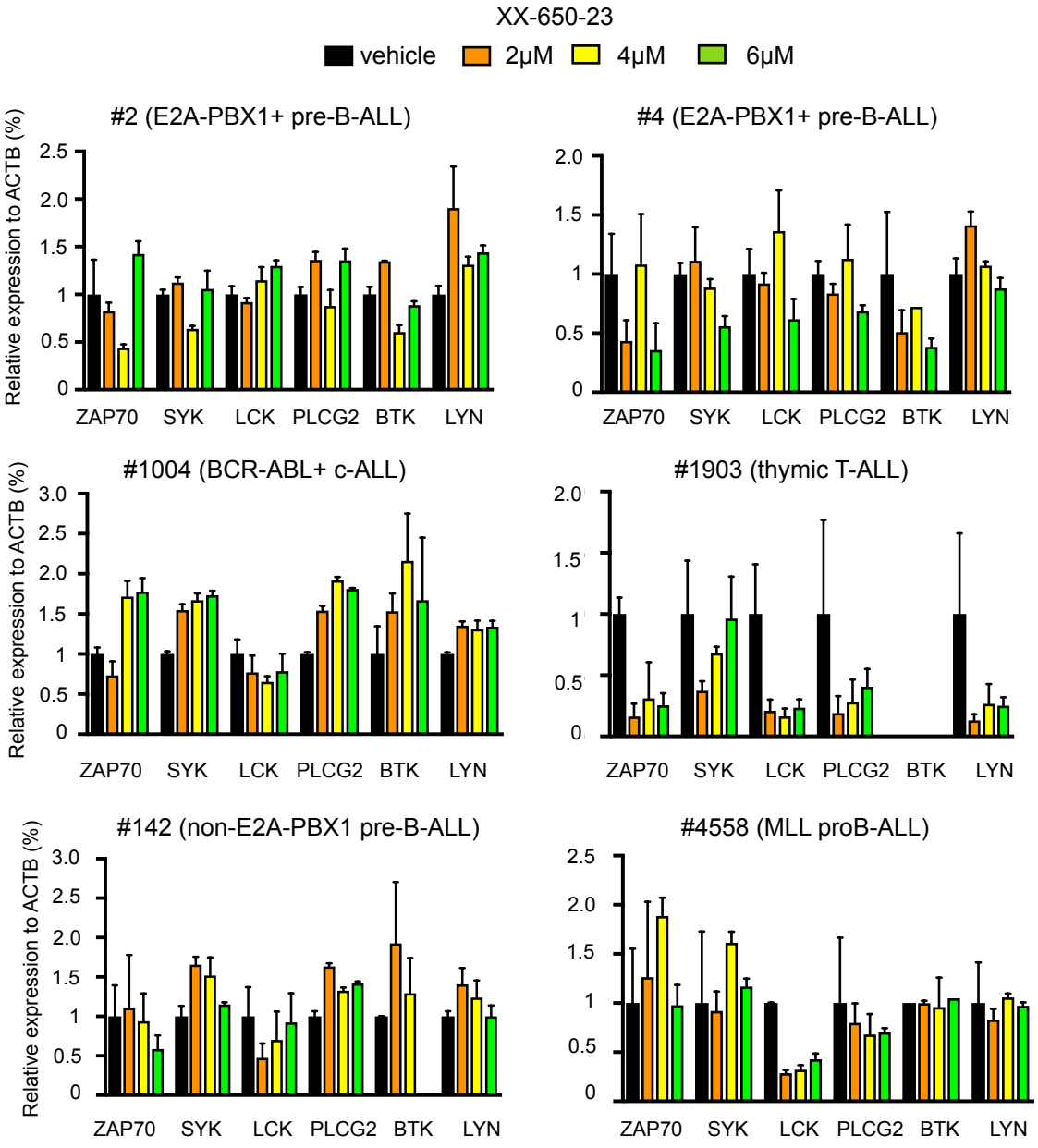

Suppl. Figure S5. Pharmacologic inhibition of CBP decreases expression of preBCR-associated genes in a selected subset of primary ALL cells. Primary ALL cells with different karyotypes and immunophenotypes were treated in vitro for 72 hrs. with XX-650-23 at indicated concentrations. Graph shows relative expression of pre-BCR –associated genes by RT-qPCR after pharmacologic inhibition of CBP. Data represent the mean ±SEM of three independent measurements.

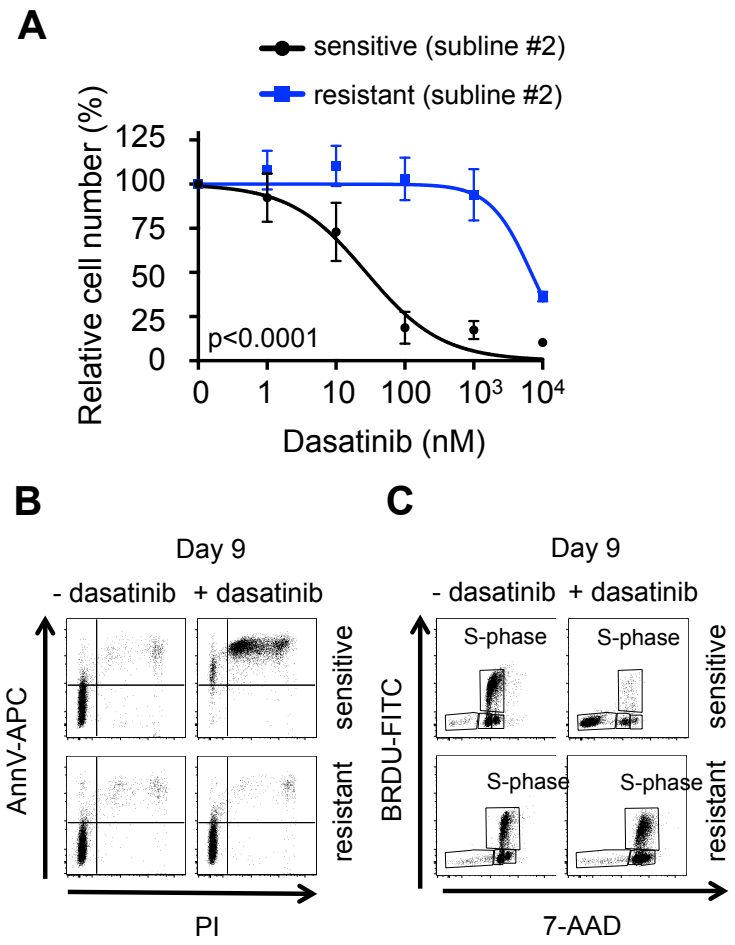

Supplementary Figure S6. Generation of dasatinib resistant pre-BCR+/E2A-PBX1+ human cells. (A) Sensitive and resistant RCH-ACV cells from a second independently generated subline were treated with increasing concentrations of dasatinib. Titration curve data represent mean ±SEM of three independent experiments. Statistical analysis by F test. **(B)** Dot plots represent annexin V/PI staining assessing apoptosis and cell death and **(C)** BRDU/7-AAD staining assessing cell cycle by flow cytometry. Dasatinib-sensitive and -resistant RCH-ACV cells were cultured in the presence of vehicle or 1 μM dasatinib for nine days. A representative of two experiments is shown.

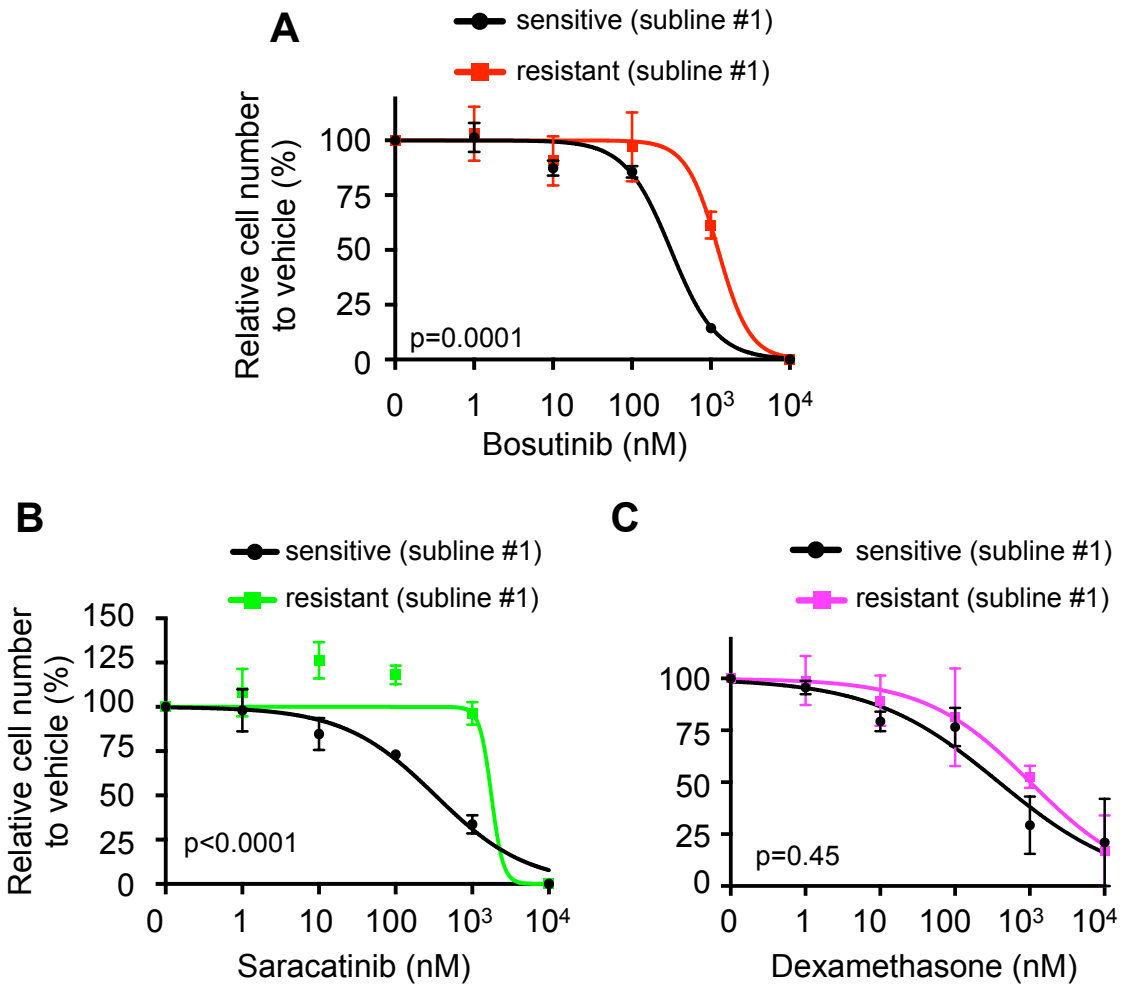

Supplementary Figure S7. Generation of dasatinib resistant pre-BCR+/E2A-PBX1+ human cells. (A) RCH-ACV sensitive and resistant cells from subline #1 were treated with the SRC family kinase inhibitors bosutinib or **(B)** saracatinib, or **(C)** the corticosteroid dexamethasone (as control). Cell proliferation was assessed after four days by trypan blue assay. Data represent mean ±SEM of three independent experiments. Statistical analysis by F test.

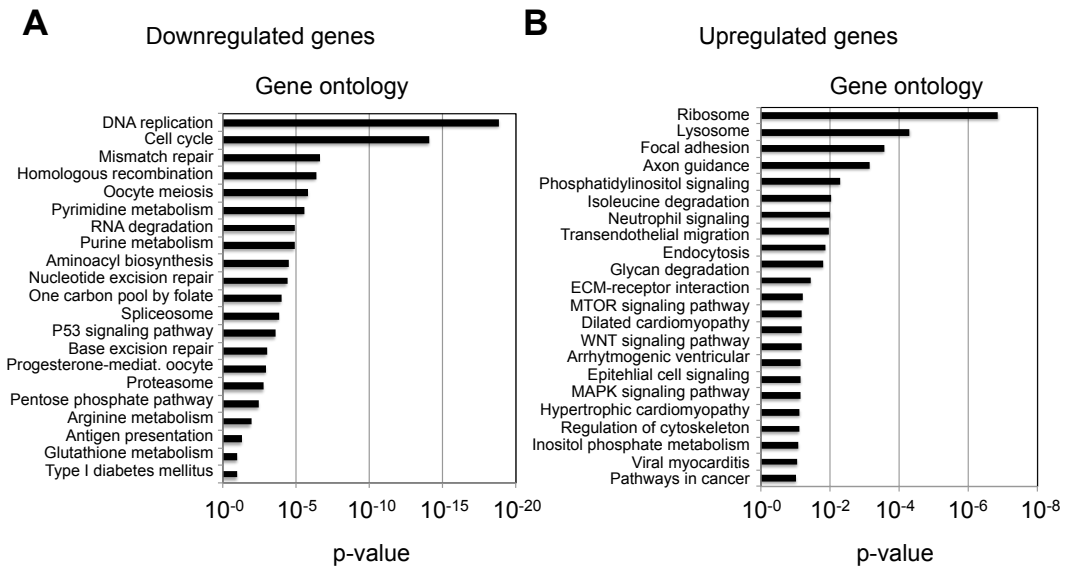

Supplementary Figure S8. Global transcriptomic analysis highlights pathways involved in dasatinib sensitivity and resistance. (A) Gene ontology analysis of KEGG pathways from common downregulated and **(B)** upregulated genes analyzed by RNAseq from generated dasatinib- sensitive and -resistant RCH-ACV sublines. Bars represent p-values of KEGG pathways enriched in the gene ontology analysis from common regulated genes in dasatinib-resistant RCH-ACV sublines.

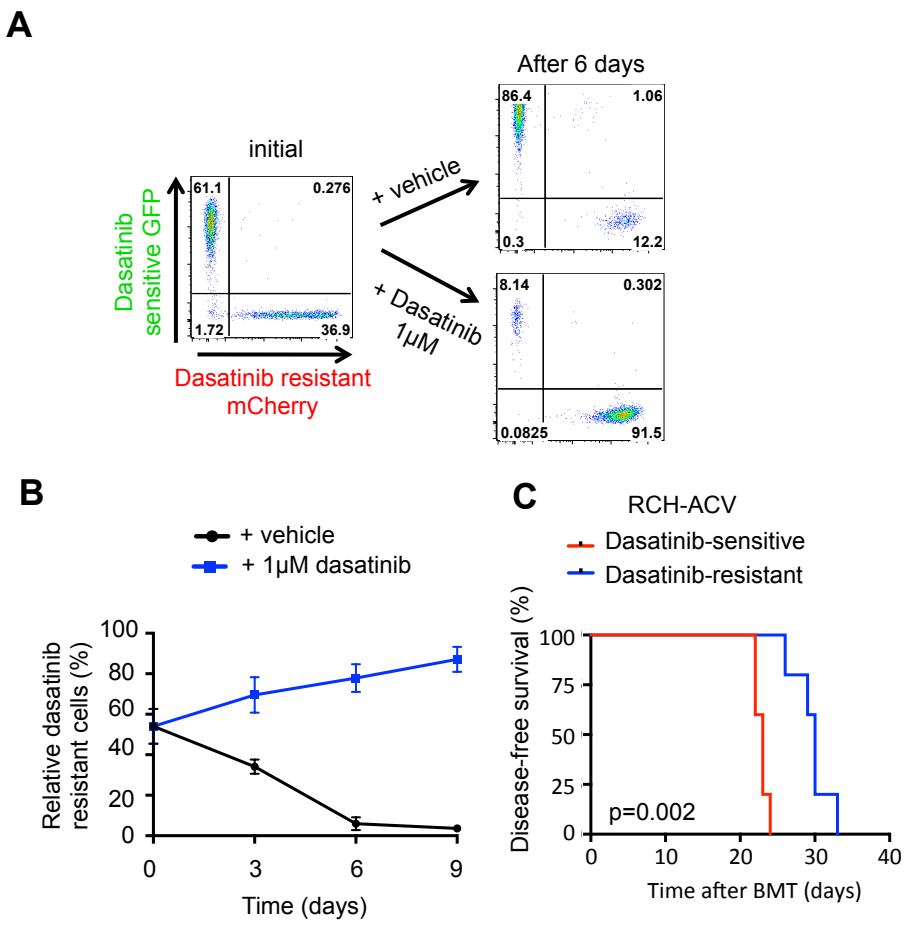

Supplementary Figure S9. Functional characterization of dasatinib-resistant cells. **(A)** Dot plots show results of competition assay between dasatinib-sensitive RCH-ACV cells transduced with shLuc-GFP vector and dasatinib resistant RCH-ACV cells transduced with shLuc-mCherry vector. After transduction and puromycin selection, cells were mixed 50/50 at day 0. Mixed cells were treated either with vehicle or dasatinib (1 μM) for six days. A representative experiment is shown. **(B)** Diagram shows the percentage of dasatinib-resistant RCH-ACV cells assessed by flow cytometry every three days. Data represent mean ±SEM of three independent experiments. **(C)** Kaplan-Meier curve shows disease-free survival of NSG mice xeno-transplanted with dasatinib-sensitive and –resistant RCH-ACV cells. Statistical analysis by log rank test. Note: these mice correspond to the vehicle-treated mice from Figure 4B.

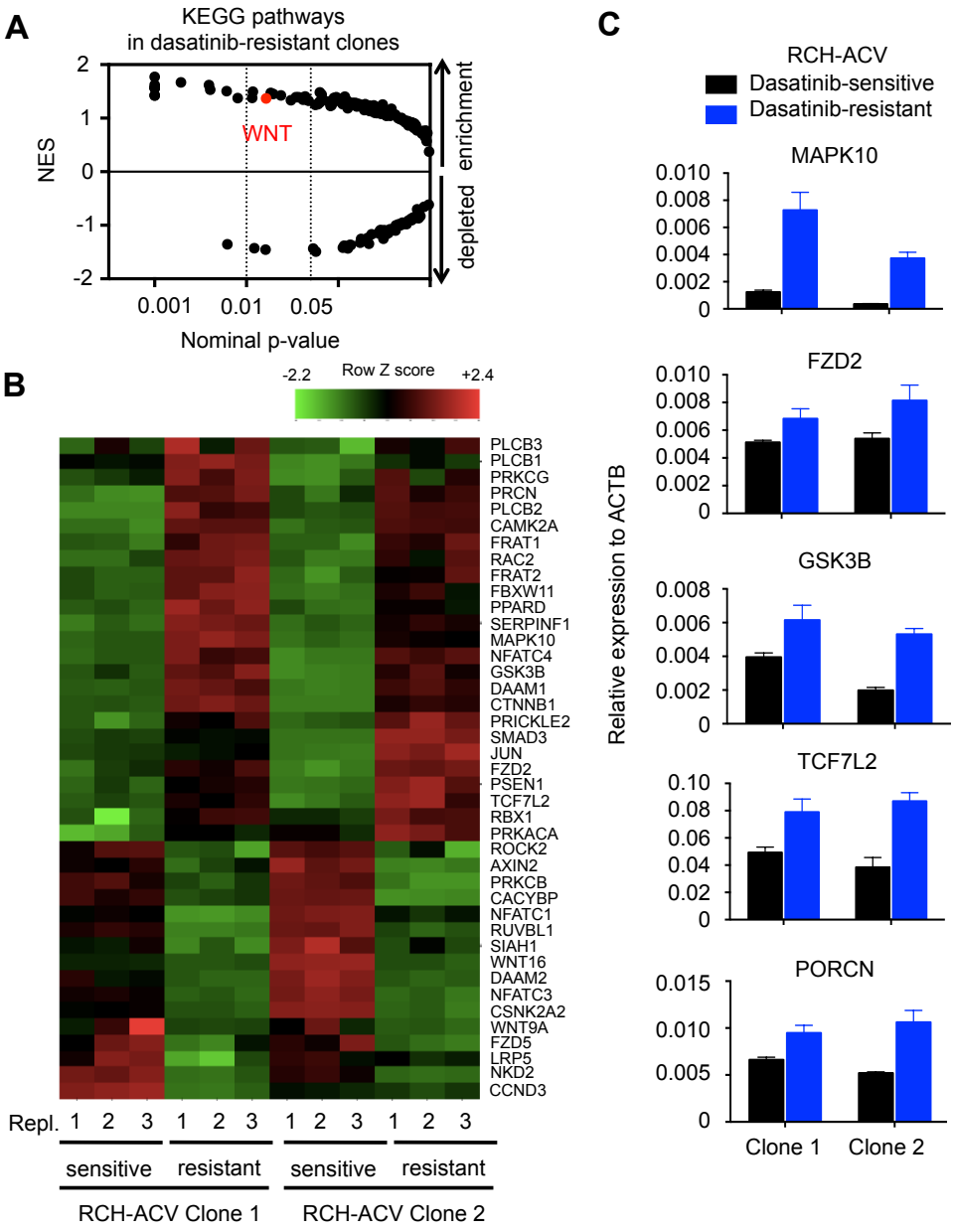

Supplementary Figure S10. Involvement of the WNT signaling pathway in acquired dasatinib resistance. (A) Gene set enrichment analysis of KEGG pathways from common regulated genes identified the WNT pathway in dasatinib-resistant sublines. NES, normalized enrichment score. **(B)** Heat map represents row Z scores of common up- and downregulated genes involved in the WNT signaling pathway from two independently generated dasatinib-sensitive and –resistant RCH-ACV sublines. Each sample was analyzed by RNA-seq in triplicate. Repl., replicate. **(C)** Validation of selected genes involved in the WNT signaling pathway and upregulated in dasatinib-resistant RCH-ACV cells by RT-qPCR. Bar denotes mean and error bars, SEM of three independent replicates. *ACTB* was used as control gene.

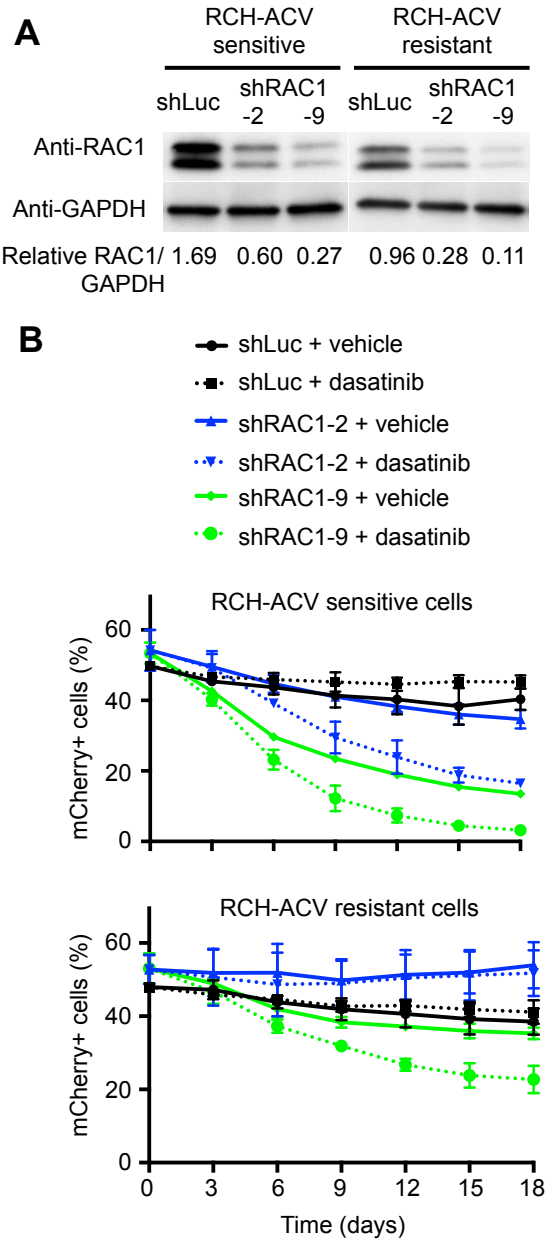

Supplementary Figure S11. Involvement of the WNT signaling pathway in dasatinib resistance. (A) Western blot shows RAC1 levels following knock-down by two different shRNA constructs in RCH-ACV sensitive and resistant cells. GAPDH represents loading control. Densitometry values shown at the bottom of the panel were calculated using Image J software. **(B)** Diagram shows percentage of mCherry+ cells transduced with shRNAs for luciferase (control) or RAC1 in the presence of vehicle or dasatinib (20 nM for dasatinib-sensitive and 1μM for dasatinib-resistant RCH-ACV cells) for 18 days. Graph show mean ±SEM of three independent experiments.

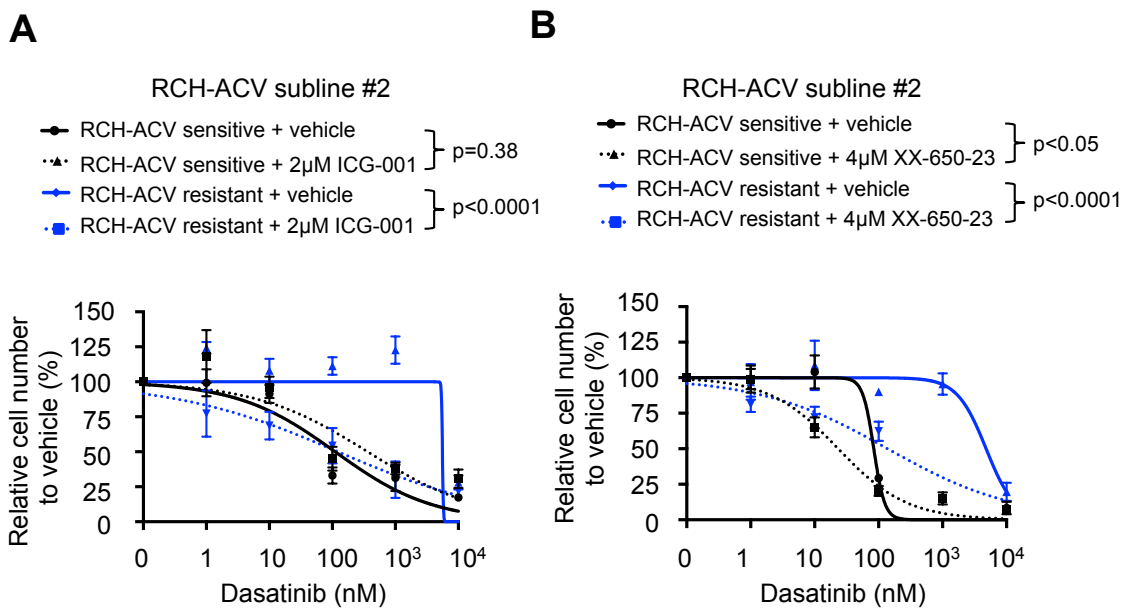

Supplementary Figure S12. CBP inhibitors restore dasatinib sensitivity in human pre-BCR+ RCH-ACV cell line. (A) RCH-ACV sensitive and resistant cells from subline #2 were treated with increasing concentrations of dasatinib in combination with either ICG-001 (2μM) or **(B)** XX-650-24 (4μM) for four days. Cell proliferation was assessed every three days by trypan blue assay. Data represent mean ±SEM of three independent experiments. Statistical analysis by F test.

Supplementary tables

Supplementary Table S1. shRNA screen candidates

See Excel file

Supplementary Table S2. shRNA sequences

Gene target	Name	Target shRNA target sequence 5'->3'
CBP	shCBP-2	AACTTGCATGCGATTCACTGGC
CBP	shCBP-3	TAAAGAAGTGGCATTCTGTTGC
RAC1	shRAC1-2	TGGGCATTTAATTCATCTTTAA
RAC1	shRAC1-9	ACCAATGCATTTCCTGGAGAAT
Luciferase	shLuc	GAGCTGTTTCTGAGGAGCC

Supplementary Table S3. sgRNA sequences

Gene target	Gene target	Target sgRNA target sequence 5'->3'
CBP	sgCBP-1	GAGCCCCCGGGGCTGGTA
CBP	sgCBP-2	GTCGGAGCTTCTACGAGG
CD38	CD38	TGTACTTGACGCATCGCGCC

Supplementary Table S4. Taqman probes used for RT-qPCR

Species	Target gene	Taqman probe (from Life Technologies)
Human	*CBP*	Hs00932905_m1
Human	*MAPK10*	Hs00373461_m1
Human	*FZD2*	Hs00361432_s1
Human	*GSK3B*	Hs01047719_m1
Human	*TCF7L2*	Hs01009044_m1
Human	*PORCN*	Hs00224508_m1
Human	*ACTB*	4352935 (Applied Biosystems)

Supplementary Table S5. SNV/Indels in RNAseq

See Excel file

Supplementary Table S6. Primers for sequencing R1748H SNV in *CBP* gene

Gene target		**Primer sequence**
CBP	FW	ACGTGTCCAATGACCTGTCC
CBP	RW	GCACGGGGCATTTGTTTTCT